

Inexpensive Interferometer for Low Frequency Radio Astronomy

Guilherme S. Rosa^{*‡}, Nelson J. Schuch^{*§}, Natanael R. Gomes^{†¶} and Renato Machado^{†||}

^{*}Southern Regional Space Research Center - INPE/MCT in collaboration with the Santa Maria Space Science Laboratory - LACESM/CT/UFSM

Santa Maria, RS 97105-900, Brazil

[‡]Email: guilherme@lacesm.ufsm.br

[§]Email: njschuch@lacesm.ufsm.br

[†]Electronic and Computing Department, Federal University of Santa Maria and Santa Maria Space Science Laboratory, Technology Center - CT/UFSM

Santa Maria, RS 97105-900, Brazil

[¶]Email: natanael@lacesm.ufsm.br

^{||}Email: renatomachado@ieee.org

Abstract—An interferometric array similar to the low frequency array (LOFAR) prototype station (LOPES) and to the eight-meter-wavelength transient array (ETA) is being developed to cover the LOFAR frequency range under 100 MHz at the Southern Space Observatory (SSO) (29.4° S, 53.8° W, 480 m. a. s. l.), in São Martinho da Serra, RS, South of Brazil. In accordance with previous observational spectrum results, the SSO site was classified as being suitable to receive sensitive and sophisticated radio interferometers, based on the phased array concept, similar to those employed at the European LOFAR stations. This paper describes the technical details of developing and implementing of a radio astronomy low cost elementary interferometer for the frequency range of 20 – 80 MHz.

I. INTRODUCTION

LOFAR is a next-generation radio telescope under construction in the Netherlands with long-baseline stations under development in other European countries. LOFAR is an emerging European sensor network with continental dimensions for space and Earth observations. The LOFAR telescope uses phased antenna arrays to form an aperture synthesis telescope for receiving radio signals in the frequency band of 30 – 240 MHz [1]-[3].

There are currently discussions with research institutions from Germany, UK, Italy, France, Poland and Sweden, aiming the installation of LOFAR stations in these countries [1]-[3]. These partnerships will extend the “wide area sensor network” and the resolution and sensitivity of the LOFAR system in Europe. The LOFAR telescope will operate in the 30 – 80 MHz and 120 – 240 MHz bands (80 – 120 MHz being dominated by FM radio broadcasting transmissions). As a predecessor to the square kilometer array (SKA) planned to be constructed after 2015, it has a broad impact on the future of Radio Astronomy and Astrophysics, which goes well beyond the current project [1].

To verify whether or not radio emission from cosmic rays is indeed detectable and useful in a modern cosmic ray experiment, [4] built the LOPES experiment. LOPES is a phased array of dipole antennas with digital electronics developed

to test same aspects of the LOFAR concept. Considering LOPES, radio emission from cosmic ray air showers at 43 – 73 MHz on a regular basis with unsurpassed spatial and temporal resolution can be detected [4].

ETA is a new radio telescope consisting of 12 dual polarized 38 MHz resonant dipole elements [5]. ETA has an array of inverted V-shaped design combined with a simple active balun that cover the range of 27 – 49 MHz [5].

The proposed interferometer is similar to LOPES and ETA methodology. The ubiquitous galactic synchrotron emission is very strong and can easily be the dominant source of noise in the observation at sub 100 MHz frequency range. Then, the sensitivity of a telescope is limited by galactic noise.

The galactic noise limited concept is also being employed in the LOFAR. As a result, [6] shows that even simple dipoles can deliver an extraordinary useable bandwidth.

The paper is organized as follows. Section II briefly describes the scientific goals of the proposed interferometer. Section III details the interferometer design. Concluding remarks are presented in Section IV.

II. SCIENTIFIC AIMS

The main objective of proposed interferometer is the development of low cost instrumentation compatible with the LOFAR methodologies.

III. INTERFEROMETER

The low cost prototype interferometer proposed here can be generically divided into three components: active antenna, analog receiver and digital correlator.

A. Active Antenna

The active antenna is compounded by a dipole radiator, a pair of amplifiers and a balun. The role of the dipole antenna is to transfer incident electromagnetic power, including the galactic noise and emissions from astronomical sources, to the amplifier input. The amplifier is the circuitry connected

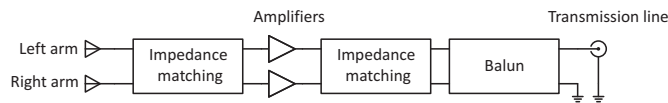


Fig. 1. Basic concept for a low frequency radio astronomy active antenna of LOFAR.

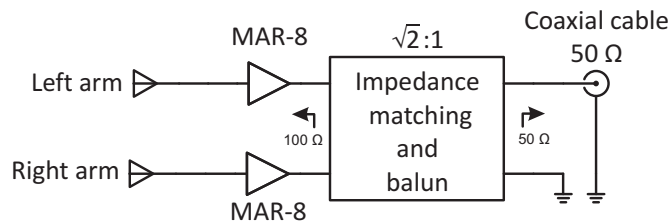


Fig. 2. An active antenna concept using two Mini-Circuits MAR-8 monolithic amplifiers.

directly to the terminals of the dipole antenna. The amplifier has as purposes: 1) set the noise temperature of the system and 2) buffer the impedance between dipole antenna and feedline.

Antennas for low frequency radio astronomy (such as dipoles [6]) are typically balanced. The coaxial cable feed lines are unbalanced, thus, is necessary a balun to transform a balanced line, in the output of the amplifiers, to an unbalanced line at the coaxial cable.

The configuration of LOFAR active antennas was presented in [3] and is shown in Fig. 1. Immediately after the dipole arms radiator, a network impedance transformer gives the impedance necessary for the matching with the amplifiers input. In the output of the amplifiers there are more two transformers: one determines the impedance of the transmission line and the other transformer unbalance the signal, i.e., the balanced line coming from the center dipole is converted into an unbalanced transmission line.

The concept presented by Tan and Rohner [3] is extremely didactic, and it is believed that its practical implementation was not performed in the LOFAR antennas. The configuration of the active antenna implemented in the proposed interferometer follows the precepts of the radio telescope ETA. According to Ellingson [5], the ETA active antenna configuration is similar to that presented by Stewart, et al. [9]. In this topology, the use of separate amplifiers reduces significantly the common mode current that could occur if the dipole is directly connected to the transformer [9].

The amplifier circuit of the prototype uses two mini-circuits MAR-8 [10] monolithic amplifiers. This device offers the basic necessities required for a low frequency active antenna according to the data sheet [10]: high gain, input and output impedances of 50 Ω, and low noise figure. The feedline uses a radio frequency (RF) coaxial cable RG-58 (50 Ω). A RF transformer determines the impedance matching between the amplifiers output and the feedline. One of transformer coil terminals, on the side of a feedline, is a grounded and unbalanced transmission line, as shown in Fig. 2.

The impedance matching and balun block (Fig. 2) is a circuit that transforms the impedance and unbalance the

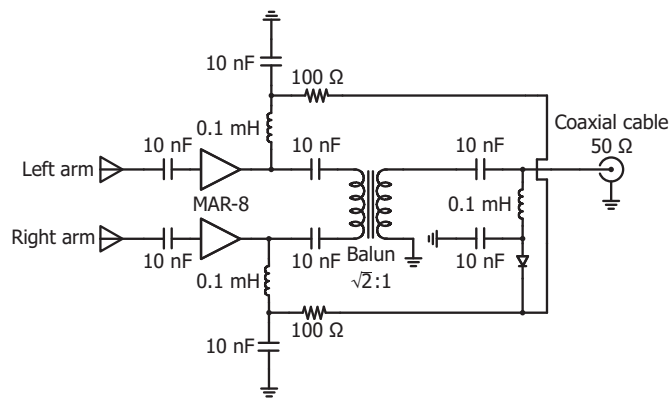


Fig. 3. The complete active antenna circuit.

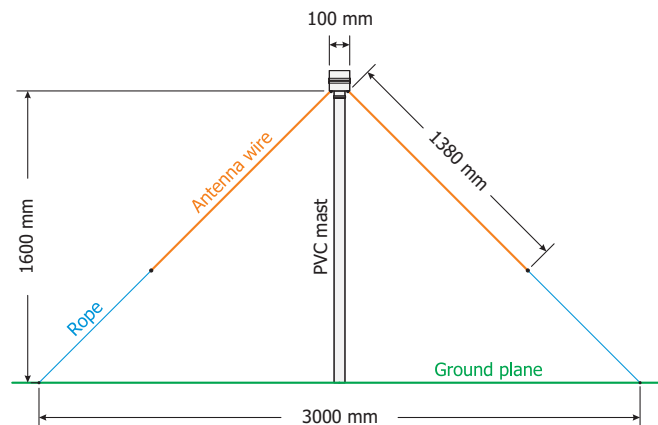


Fig. 4. A LOFAR LBA like, proposed in [11].

transmission line. Fig. 2 shows a transformer with voltage transformation ratio of $\sqrt{2} : 1$ in order to check the impedance matching between the output of the amplifiers and the coaxial cable input. The equivalent input impedance of the transformer is 100 Ω – it results of the amplifiers impedance output (50 Ω in series with 50 Ω). The equivalent impedance at the transformer output is 50 Ω; it is the same impedance of the coaxial cable. The complete circuit of the active antenna is shown in Fig. 3.

The power of the amplifiers is performed through a bias tee circuit. Thus, in the coaxial cable exists a direct current (DC) signal – inserted into the receiver – and a RF signal – that is provided by the balun output. At the receiver there is a bias tee identical in order to filter DC and RF signals.

The LOFAR low band antenna (LBA) frequency range is from about 10 MHz (near the ionosphere cut-off frequency) to 80 MHz [11]. To operate successfully in this frequency range an inverted V dipole antenna is used with a ground plane reflector, as shown in Fig. 4. According to van Cappellen, et al. specifications [11], the dimensions of the antenna of Fig. 4 show a LOFAR LBA, with resonance frequency around 52 MHz. The complete active antenna circuit is located at the top of the PVC mast (Fig. 4) which is directly connected to the dipole wire arms.

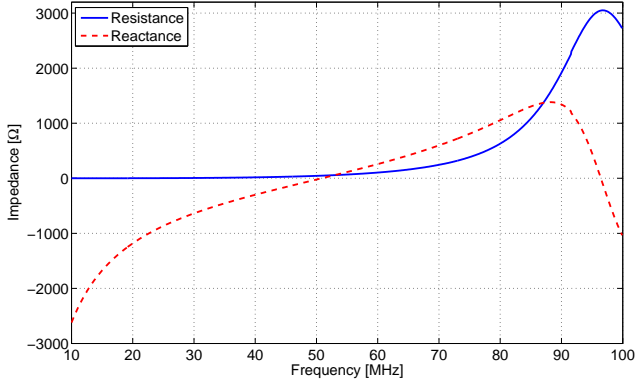


Fig. 5. NEC-2 simulated impedance for the antenna shown in Fig. 4 using a realistic ground.

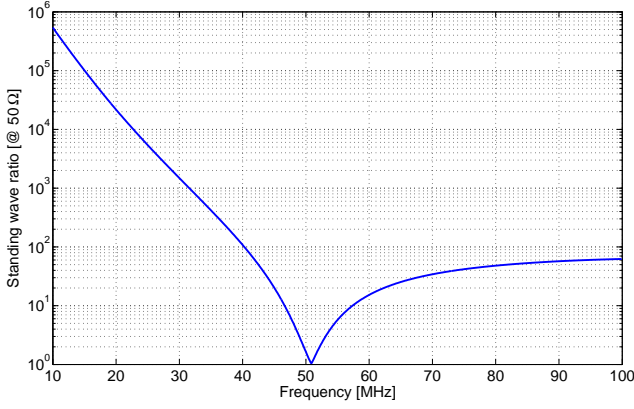


Fig. 6. NEC-2 simulated standing wave ratio for the antenna shown in Fig. 4 using a realistic ground.

A simple inverted V-shape dipole was constructed with 1 mm copper wire. This antenna was analyzed using NEC-2 based method of moments (MM) and using finite element method (FEM) employed by HFSS software. Two ground sceneries were considered: 1) realistic lossy ground having conductivity of $\sigma = 5 \times 10^{-3} S/m$ and relative permittivity $\epsilon_r = 13$, and 2) perfectly-conducting ground, approximating the use of wire mesh in the ground under antenna to mitigate the loss.

The simulation results of impedance and standing wave ratio for the dipole antenna (shown in Fig. 4) using a realistic ground are presented in figures 5 and 6. These results are for the worst case found in the simulations: NEC-2 with realistic ground.

The usable bandwidth of the active antenna is one in which the galactic noise dominates the instrumentation noise. The model proposed by Cane [12] for the galactic noise background was employed to evaluate the usable galactic noise limited bandwidth.

1) *Galactic noise model*: The galactic noise power can be described in terms of the intensity I_ν integrated over the antenna pattern. The resulting power spectral density at the terminals of an antenna is given by

$$S_a \approx \frac{1}{2} \int I_\nu A_e d\Omega [W Hz^{-1}] \quad (1)$$

where A_e is the antenna effective aperture, the integration is over solid angle, and the factor of 1/2 is due to the fact that any single polarization captures about half of the available power since galactic noise is unpolarized [6].

The galactic noise intensity can be modeled as being spatially uniform and filling the beam of the antenna. A requirement for the low frequency radio astronomy antennas is that they have very broad beamwidth [6], such that is approximately constant over most of the sky. Assuming antenna gain very small at and below the horizon, (1) can simplify to

$$S_a \approx \frac{1}{2} I_\nu A_e \Omega [W Hz^{-1}] \quad (2)$$

where Ω is beam solid angle.

The gain of the antenna is given by

$$G = e_r D \quad (3)$$

where D is directivity and e_r is efficiency. In this analysis, mechanisms which make $e_r < 1$ include loss due to the finite conductivity of the materials used to make the antenna, and the imperfect ground. Since

$$A_e = \frac{\lambda^2}{4\pi} G \text{ and } \Omega = \frac{4\pi}{D} \quad (4)$$

where $A_e \Omega = e_r c^2 / \nu^2$, ν is frequency and c is the speed of light. Therefore

$$S_a \approx \frac{1}{2} e_r I_\nu \frac{c^2}{\nu^2}. \quad (5)$$

Equation (5) will be useful to express the power density in terms of an equivalent temperature. This is possible using the Rayleigh-Jeans law

$$I_\nu = \frac{2\nu^2}{c^2} k T_{sky} \quad (6)$$

where k is Boltzmann's constant ($1.38 \times 10^{-23} J/K$), and T_{sky} is defined to be the antenna equivalent temperature corresponding to galactic noise. Thus, (5) can be written

$$S_a \approx e_r k T_{sky} \text{ where } T_{sky} = \frac{1}{2k} I_\nu \frac{c^2}{\nu^2}. \quad (7)$$

An approximation for I_ν can be obtained from [12], which quantified the spectrum of the galactic noise background based on observations of the Galaxy polar regions at four frequencies between 5.2 and 23.0 MHz. From these measurements, it was determined that the intensity is given in units of $W m^{-2} Hz^{-1} sr^{-1}$ by

$$I_\nu = I_g \nu^{-0.52} \frac{1 - e^{-\tau(\nu)}}{\tau(\nu)} + I_{eg} \nu^{-0.80} e^{-\tau(\nu)} \quad (8)$$

where $I_g = 2.48 \times 10^{-20}$, $I_{eg} = 1.06 \times 10^{-20}$, $\tau(\nu) = 5.0 \nu^{-2.1}$, and for this case, ν is frequency in MHz. I_g and I_{eg} are the coefficients obtained by Cane in [12], and this result has been successfully used to calibrate telescopic observations

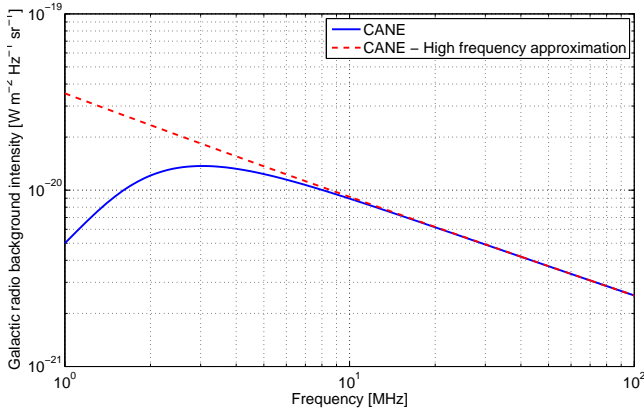


Fig. 7. Galactic noise intensity. Solid blue line: Cane model. Dashed red line: approximation of Cane for high frequencies.

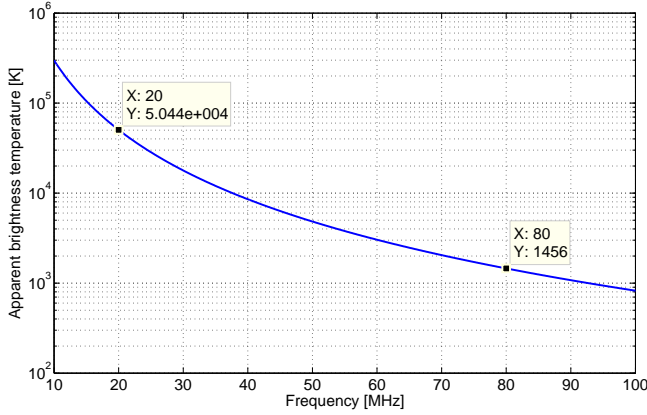


Fig. 8. Antenna brightness temperature received by a low-gain antenna, as a function of frequency using the Cane high frequency galactic noise model.

of great field vision [6]. The above expression is given in units of steradian (sr), i.e., measures the current on a solid angle.

In (8), the first term applies to the contribution of the galaxy itself, whereas the second term is due to extragalactic noise, which is assumed to be spatially uniform.

In Fig. 7, it is possible to note that for the spectrum above 10 MHz (8) can be simplified to

$$I_\nu \approx I_g \nu^{-0.52} + I_{eg} \nu^{-0.80}. \quad (9)$$

The result in (9) applies to the Galaxy poles since the noise intensity is correlated with the distribution of mass in the Galaxy, a result which represents a minimum range, while the noise in the direction of the galactic plane is somewhat larger. However, as the galactic plane remains spatially unresolved at low gain antennas, the additional contribution of noise is relatively small [6].

The Cane high frequency galactic noise model, given by (9), is used throughout this paper. Thus, the performance of antennas is somewhat underestimated. Equations (8) and (9) are represented as a function of frequency in Fig. 7.

The value of T_{sky} is diagrammed in Fig. 8, using the Cane approximation for high frequency. Figure 8 highlights

the antenna temperature of the extremes frequency of interest: at 20 MHz worth around 50000 K and 80 MHz worth about 1500 K.

According to the results proposed in Fig. 8, the noise temperature of the whole active antenna cannot exceed 1500 K at 80 MHz.

2) *Galactic noise limited bandwidth*: The main requirement of the active antenna system is that it provides a signal to the receiver where the dominant noise is the unavoidable galactic noise.

The determination of the degree which the receiver input is limited by the galactic noise requires knowledge of the noise temperature system contributions.

The active antenna system was modeled considering the galactic noise and the instrumental noise. The instrumental noise is formed by the noise temperature contribution of pre-amplifier and the transmission line.

According to [6], the ground noise can be neglected, since in practice, the soil tends to behave more as a spotlight than as a body.

The man-made noise is the background noise radio frequency aggregate resulting from human activity, which is known to exhibit noise-like spectra. This noise is characterized in [15] and applies a multiplication factor to the galactic background noise. This factor varies from 5 to 30. However, as the rating for this factor depends on the site location and the spectral characteristics of observation region, the contribution of man-made background noise will be neglected. Thus, the performance of antennas is somewhat underestimated.

The contribution of temperature due to the galactic noise is the power spectral delivered to the receiver. Let S be the power spectral density of the signal associated with T_{sky} at the output of feedline. Given the Cane [12] galactic model for the system, S becomes

$$S = e_r k T_{sky} (1 - |\Gamma|^2) G_{pre} G_f. \quad (10)$$

where $(1 - |\Gamma|^2)$ represents the fraction of power available at the antenna which is successfully transferred to the preamplifier. This fraction is nominally 1, but is often much smaller than one due to impedance mismatch between the antenna and amplifier.

Γ is the voltage reflection coefficient on the antenna terminals looking into the preamplifier and is given by

$$\Gamma = \frac{Z_{pre} - Z_a}{Z_{pre} + Z_a}. \quad (11)$$

The preamplifier noise as measured at the input of receiver can be defined in terms of the preamplifier input-referenced noise temperature T_{pre} as

$$N_{pre} = k T_{pre} G_{pre} G_f. \quad (12)$$

Finally, the noise resulting from the transmission line loss can be significant. The noise at the end of the feedline can be described in terms of the physical temperature T_{phys} as

$$N_f = k T_{phys} (1 - G_f). \quad (13)$$

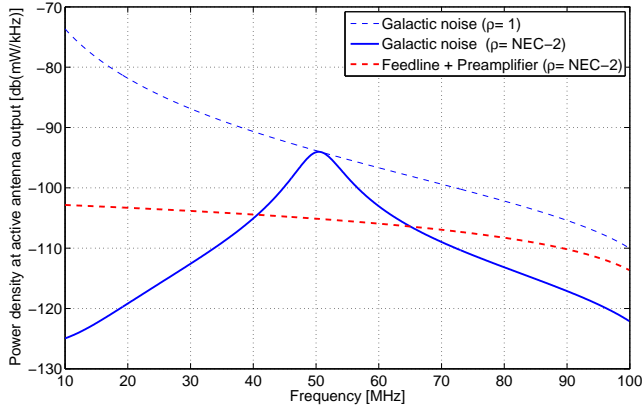


Fig. 9. Comparison between the instrumental active antenna noise (dashed-strong red) and the galactic noise (solid-strong blue). The noise due to a system with standing wave ratio equal to 1 (perfect impedance matching) is represented by the dashed line.

The ratio γ of galactic noise to instrumental noise measured at receiver input is given by

$$\gamma = \frac{S}{N_p + N_f}. \quad (14)$$

The noise temperature of preamplifier used to determination the bandwidth galactic noise limited was $T_{pre} = 360 K$. The amplifiers gain used was $G_{pre} = +45 dB$.

The transmission line considered was a 100 m RG-58 coaxial cable. The operating temperature chosen was $T_{phys} = 240 K$ (20 °C) with a gain associated with the transmission line (coaxial cable RG-58) ranging from -4.8 dB to -15.6 dB, between 10 and 100 MHz respectively.

The comparison between the instrumentation active antenna noise (feedline and preamplifier) and the galactic noise is shown in Fig. 9. According to Fig. 9, we can conclude that the active antenna operates limited by the galactic noise in the frequency range about 41 – 65 MHz.

B. Analog Receiver

The new generation of radio telescopes like the LOFAR, long wavelength array (LWA) and SKA is composed by thousands of antennas spread over stations (which are formed by tens of antennas) that cover continental extensions [6], [7]. The amount of receptors is directly proportional to the number of antennas. Therefore, it is evident the interest in reducing the cost of RF receivers used in large radio telescope.

The use of classic RF receivers, such as the superheterodyne receiver topology, results in high costs for large interferometers. The proposed interferometer employs two super-regenerative receivers deployed for low frequency radio astronomy applications. According to [8], the super-regenerative receiver has a reduced cost and a low power consumption. The receiver prototype is a hybrid model of software-defined radio (SDR), because its output signal is at audio frequency, and also due the interferometer correlation is performed by software.



Fig. 10. Receiver topology.

The frequency range of the receiver described here is 20 – 80 MHz. The proposed receiver employs the super-regenerative topology motivated primarily by the low cost of this type of receiver.

In order to overcome the major problems present in the super-regenerative receiver architecture [13], it was proposed a receiver topology composed by: 1) a bias tee, 2) an impedance matching network for 20 – 80 MHz, 3) a super-regenerative receiver and 4) an audio amplifier stage, as shown in the block diagram of Fig. 10.

Bias tee block is used to feed the active antenna amplifiers and its design and operation details are shown in [18]-[19], moreover, their components are equal to the bias tee located in active antenna. It is important to mention that the employed bias tee does not insert significant noise in the RF signal and does not significantly alter the impedance of receiver input. Therefore, the electrical analysis of bias tee circuit can be overlooked.

The impedance matching network for 20 – 80 MHz was designed from impedance measurements at the receiver input. Figure 11 shows the initial values of the reflection coefficient $\Gamma_{initial}$ (normalized to 50 Ω) measured as a function of frequency. It can see that the characteristic of the reflection coefficient, and consequently the receiver impedance input is highly nonlinear and presents very high values, with a maximum of 0.95 for Γ .

The possibility of using classical techniques of impedance matching, either with network L, Pi or T [18]-[19] was discarded. According to [19], Pi and T networks are extremely narrow-band and L network is best suited for smaller values of quality factor Q, which is inversely proportional to bandwidth. [19] affirms that the cascading of multiple networks L, following several design parameters, can minimize the Q factor of a network. However, despite increasing the bandwidth, this technique has some weaknesses: the impedance matching will always be optimized to a center frequency design and the signal will be degraded in the periphery of the central frequency. Tens of cascaded L networks would be required to obtain a impedance matching for a bandwidth of 60 MHz (20 – 80 MHz) and the values for the network components can be impracticable as the number of cascaded networks increase very much.

Furthermore, in case of the proposed receiver, the design of multiple cascaded L networks would be designed to the impedance at center frequency (50 MHz), ignoring the large variations of receiver input impedance, as shown in Fig. 11.

The frequency response of the impedance matching of a simple L network is shown in Fig. 12, and it is evident that this impedance matching technique is not applicable to the receiver proposed here. The impedance matching network was designed from the input impedance measurements in the super-

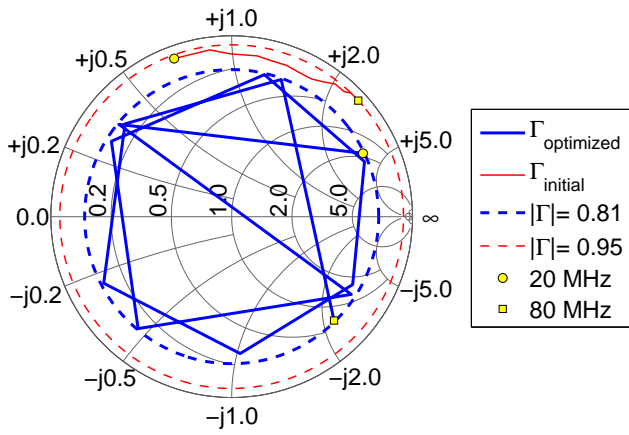


Fig. 11. Reflection coefficient measured (solid red) without the impedance matching network; reflection coefficient using the impedance matching network (solid-strong blue), the maximum value of the reflection coefficient modulus measured (dashed red) and maximum reflection coefficient modulus of the optimized network (dashed-strong blue). The reflection coefficients are normalized to 50 Ω .

regenerative receiver block.

An iterative algorithm was implemented to minimize the module of reflection coefficient $\Gamma_{initial}$ measured at the receiver input from the insertion of an LC network: a 5th order bandpass filter was chosen for the filter network. The impedance response results using the optimized matching network are shown in Fig. 11. The broadband impedance matching network circuit is shown in Fig. 14, along with the full proposed receiver circuit.

From the results shown in Fig. 12, it can be observed the occurrence of a distortion of the frequency response of the Chebyshev filter which served as the initial value for the network elements. The inductor L5, see Figure 14, was unnecessary: after network optimization the inductor value became nearly zero. The impedance matching components values are shown in detail in Fig. 14.

Through the network impedance matching was possible to limit the attenuation of the initial super-regenerative receiver that had an attenuation exceeding 10 dB with ripple of 3.5 dB for a frequency response with maximum attenuation of 4.5 dB and ripple of 0.5 dB, as shown in Fig. 12.

The super-regenerative receiver considered in the block diagram in Fig. 10 follows the operation line of the circuit integrated (CI) MK484 (see Figure 13), a high sensitivity amplitude modulation (AM) receiver [16]. However, according to MK484 data sheet [16], this CI has an input operating frequency between 150 kHz – 3 MHz. Thus, as in the absence of a low-cost CI that operates in the frequency range of interest (20 – 80 MHz), a receiver was developed with transistor logic using the same MK484 concept. The transistors used in the receiver shown in Fig. 14 are general purpose BC548 NPN transistor, which has a typical operating frequency of up to 150 MHz [17].

The last step of the basic topology of the receiver is the audio amplifier. This step was performed with an OPA277PA

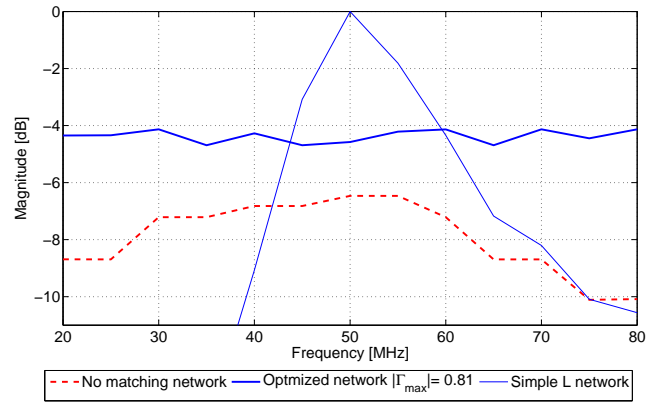


Fig. 12. Frequency response of the magnitude of power delivered to the receiver input: 1) without the impedance matching network (dashed red), 2) using the optimized impedance matching network (solid-strong blue) and 3) using a single L network (solid blue).

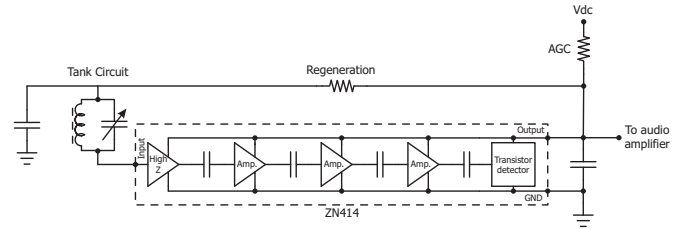


Fig. 13. Basic circuit receiver using the MK484. Adapted from MK484 data sheet [16].

operational amplifier. The CI was fed asymmetrically (to limit the amplifier output voltage to values compatible with the maximum permissible limits of the computer sound card used in correlation data acquisition step). The complete circuit is shown in detail in Fig. 14.

C. Digital Correlator

The main digital correlator topologies employed in Radio Astronomy are: XF and FX [11]. Overall, the XF and FX correlators are very similar. The main difference is that the correlation (symbolized by X) in the topology XF is performed before the Fourier transform (denoted by \mathfrak{F}). In the FX topology, the order of operations is reversed: first the signals are carried to the frequency domain, and subsequently carried out the correlation.

According to [3], the topology used in LOFAR correlator is the FX. The proposed digital correlator is still in testing. During this step, a PC sound board was used as A/D converter. The receiver outputs were connected to a sound board computer, running acquisition software to storage the data.

The software saves the amplitudes of each channel of the entrance of the PC sound card along with the acquisition time. These data are written to a text file, and later of acquisition, through a mathematician software data processing, such as MatLab or GnuOctave is performed the correlation. The response of this step is proportional to the visibility function of a monitored source.

